Korean J. Chem. Eng., **20**(5), 922-929 (2003)

Adsorption and Desorption Dynamics of Amino Acids in a Nonionic Polymeric Sorbent XAD-16 Column

Woo Chul Yang, Wang Geun Shim, Jae Wook Lee* and Hee Moon†

Faculty of Applied Chemistry, Chonnam National University, Gwangju 500-757, Korea
*Department of Chemical Engineering, Seonam University, Namwon 590-170, Korea
(*Received 27 June 2003 • accepted 28 July 2003*)

Abstract−A separation technique for amino acids, phenylalanine and tryptophan, from aqueous solution was studied in a column that was packed with a polymeric resin, XAD-16. This technique is based on a cyclic operation that has three typical steps such as adsorption, desorption, and washing. In particular, the desorption step for amino acids from the resin was carried out by using organic solvents, isopropyl alcohol and methanol. The desorption mechanism was assumed to be a competitive adsorption between amino acids and solvents, and the ideal adsorbed solution theory (IAST) based on the Langmuir equation as a single component isotherm was used in describing multicomponent equilibria. Adsorption and desorption breakthrough curves of the two amino acids were measured under various experimental conditions such as concentration, flow rate, and column length, in order to check the feasibility of the resin as a medium for the separation of amino acids. It was found that this separation technique could be a promising one for this purpose. Also, a simple dynamic model was formulated to describe both adsorption and desorption breakthrough curves of amino acids.

Key words: Adsorption Isotherm, Amino Acids, Column Separation, Polymeric Adsorbents, Regeneration

INTRODUCTION

Amino acids have acquired an important role in the pharmaceutical, food, and health product industries. They have been produced by selective fermentation through appropriate bacteria based on the high temperature acid hydrolysis of protein containing substrates [Carta et al., 1998; Doulia et al., 2001]. This technique usually yields multicomponent mixtures containing amino acids, inorganic ions, and high molecular weight compounds. Typically, high molecular weight compounds are removed by centrifugation, ultrafiltration, and adsorption on activated carbons while the removal of the inorganic ions and the extraction of the individual amino acids are carried out by chromatographic techniques [Melis et al., 1996; Moitra et al., 1998].

To improve the efficiency of recovery, separation, and purification from fermentation broths, several separation techniques have been employed. Considering energy efficiency, selectivity, and cost, the adsorption-based separation technique is a promising method for the separation of amino acids. Several works have been reported in the literature for amino acid adsorption on various adsorbents including activated carbon, silica, ion exchangers, and polymeric resins, *etc*. [Carta et al., 1998; Doulia et al., 2001; Dutta et al., 1997; Grzegorczyk and Carta, 1996; Kubota et al., 1996]. Among them, a polymeric resin is more attractive than other media because of its regeneration characteristics. For this purpose, the separation process, which consists of three steps: adsorption, desorption, and washing, has been applied. Although polymeric adsorbents have lower adsorption capacities than other common adsorbents such as activated carbon and ion exchangers, they have much better desorption or regeneration characteristics in cyclic operations [Costa and Rodriques, 1985; Diez et al., 1998; Lee et al., 1997a; Podlesnyuk et al., 1999]. Unlike ion exchangers, polymeric adsorbents also could be applied in thermal swing adsorption, and desorption with organic solvents yields high purity.

For efficient separation and purification of amino acids from broths that contain many components, it is essential to understand the physical and thermodynamic characteristics of their adsorption and desorption on nonionic polymer resins. Therefore, our major concern in the present study was the acquisition of accurate information on adsorption equilibrium and mass transport data to quantitatively analyze adsorption and desorption behaviors of amino acids on a nonionic polymeric resin, XAD-16. Since desorption in this case can be assumed to be a competitive adsorption between amino acids and a desorbate, the ideal adsorbed solution theory (IAST) based on the Langmuir equation as a single-component equilibrium isotherm was used in describing multicomponent equilibria [Myer and Prausnitz, 1965]. A simple dynamic adsorption model was also formulated by incorporating the IAST with the mass balance equation in the column. The adsorption and desorption breakthrough curves were compared with the simulation results predicted by the model.

THEORETICAL APPROACH

1. Dynamics Model Description Based on Surface Diffusion

A dynamic model for adsorption of amino acids in the fixed-bed charged with a nonionic polymeric sorbent was formulated according to the following general assumptions: (1) The system is isothermal, (2) The shape of resin particles is spherical, (3) The column is homogeneously packed, (4) The pore size distribution is homogeneous, (5) The pore structure inside particles is uniform, (6) The fluid physical properties remains constant, (7) The flow pat-

†To whom correspondence should be addressed.
E-mail: hmoon@chonnam.ac.kr

tem is a plug flow with a constant linear velocity along the column, and (8) The surface diffusivities within the adsorbent do not vary. Under these assumptions, the transport equation inside a spherical adsorbent particle may be described by the following equation:

$$\frac{\partial q_i}{\partial t} = D_{si}\left(\frac{\partial^2 q_i}{\partial r^2} + \frac{2}{r}\frac{\partial q_i}{\partial r}\right) \tag{1}$$

with initial and boundary conditions:

$$q_i = q_i(0, r) \tag{2}$$

$$D_{si}\rho_p \left.\frac{\partial q_i}{\partial r}\right|_{r=R} = k_f(C_i - C_{si}) \tag{3}$$

$$\left.\frac{\partial q_i}{\partial r}\right|_{r=0} = 0 \tag{4}$$

The mass balance equation in the column and the relevant initial and boundary conditions are:

$$\frac{\partial C_i}{\partial t} = D_L\frac{\partial^2 C_i}{\partial z^2} - v\frac{\partial C_i}{\partial z} - \frac{1-\varepsilon_b}{\varepsilon_b}\frac{3k_f}{R}(C_i - C_{si}) \tag{5}$$

$$C_i = C_i(0, z) \tag{6}$$

$$D_L\left.\frac{\partial C_i}{\partial z}\right|_{z=0} = -v(C_i|_{z=0} - C_{fi}(t)|_{z=0}) \tag{7}$$

$$\left.\frac{\partial C_i}{\partial z}\right|_{z=L} = 0 \tag{8}$$

2. Numerical Method

In this study, the classical procedure of orthogonal collocation combined with the high accuracy of the finite element method (FEM) was applied. The entire column is at first divided into a finite number of elements, in which the space variables are discretized [Villadsen and Michelsen, 1978; Lee et al., 1997; Lee and Moon, 1998; Park, 2002]. Using the orthogonal collocation method on FEM, the resulting equations constitute a set of algebraic first-order ordinary differential equations as written in Eqs. (9) and (10).

$$\frac{\partial q_i^{(L)}}{\partial \tau} = \gamma^{(L)}\left[\sum_{j=1}^{NTS-1}\left(6AS_{i,j} - \frac{6AS_{i,NTS}}{AS_{NTS,NTS}}AS_{NTS,j}\right)q_j^{(L)} + \sum_{j=1}^{NTS-1}\left(4X_iBS_{i,j} - \frac{4X_iBS_{i,NTS}}{AS_{NTS,NTS}}AS_{NTS,j}\right)q_j^{(L)} + \frac{(4X_iBS_{i,NTS} + 6AS_{i,NTS})}{AS_{NTS,NTS}}\frac{\beta^{(L)}}{2}(C_i^{(L)} - C_{i,s})^{(L)}\right] \tag{9}$$

$$\frac{\partial C_i^{(k)^{(L)}}}{\partial \tau} = \frac{\theta\eta}{Pe\Delta Z_k^2}\left[\{BF(k,i,1) - Pe\Delta Z_k AF(k,i,1)\}C_1^{(k)^{(L)}} + \{BF(k,i,NTF) - Pe\Delta Z_k AF(k,i,NTF)\}C_{NTE}^{(k)^{(L)}} + \sum_{j=2}^{NTF-1}\{BF(k,i,j) - Pe\Delta Z_k AF(k,i,j)\}C_j^{(k)^{(L)}}\right] \tag{10}$$

where i, j are the collocation numbers within the particle or along the column. L and k are indices for the component and the section of the column, respectively. The dimensionless variables and nomenclatures have already been listed in details in our previous reports [Lee et al., 1997a, b]. The surface concentration can be determined from the corresponding isotherm or multicomponent equilibrium theories. Owing to the system stiffness, its integration is made by means of a stiff solver: LSODI of the International Mathematics and Science Library (IMSL). Inserting surface concentration into Eqs. (9) and (10), these ordinary differential equations for two vectors $\partial C_i^{(k)}/\partial\tau$ and $\partial q_j^{(k)}/\partial\tau$ are simultaneously integrated with respect to τ by using the integrating package which employs the variable-step size, variable-order, and predictor-corrector techniques that are suitable for stiff equations.

EXPERIMENTAL

The polymeric adsorbent used in this study was XAD-16. It is a macroreticular and spherical polystyrene resin cross-linked with divinylbenzene which was supplied by Rohm and Haas Co. (France). The physical properties of XAD-16 used are given in Table 1. The water content of fully swollen resin particles was determined from the weight loss of samples that occurred during drying in a vacuum oven at 383.15 K for 72 h. The arithmetic average particle diameter was determined by sorting wet resin particles with the aid of an optical microscope. It was about 635 μm. Nitrogen adsorption/desorption was measured with an ASAP-2010 volumetric adsorption apparatus (Micrometrics) at 77.4 K. The surface area was calculated by the BET method. The pore diameter was obtained from the BJH pore size distribution method. Two amino acids, L-phenylalanine (Phe) and L-trytopan (Trp) were obtained from Junsei Co. (Japan). The properties of these amino acids are shown in Table 2. The amino acids are usually amphoteric. They exist both as anions and cations, depending on the solution pH. Amino acids studied here have isoelectric points of 5.5 for Phe and 5.9 for Trp. Methanol and isoproply alchol (IPA) were used as organic desorbates in this study. Samples with purity greater than 99% were ob-

Table 1. Properties of XAD-16

Adsorbent	Unit	XAD-16
Chemical structure	-	Polystyrene
Particle size	μm	560-710
Particle density	kg/m^3	501
Particle porosity	-	0.51
Bed density	kg/m^3	244
Moisture holding capacity	%	68.96
Surface area (BET)	m^2/g	920 (≥800*)
Average pore diameter	nm	8.54
Specific gravity*	-	1.015-1.025

*from the manufacturer's report.

Table 2. Properties of model compounds used

Compound	Structure	MW	Solubility (kg/m^3)
Phenylalanine	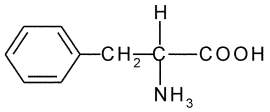	165.2	29.6
Tryptophan	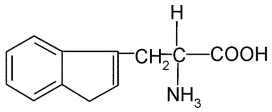	204.23	12

tained from Carlo Erba (USA).

Prior to experiments, the adsorbent was leached with isopropyl alcohol for 24 h to wet internal pores. Adsorbent particles were loaded in a 0.02 m ID glass column, and a ten-bed volume of sodium hydroxide (0.1 N) and HCl (0.1 N) was passed through the column successively at a flow rate of 1.0×10^{-4} m^3/min in order to remove impurities. Finally, a twenty bed-volume of distilled and deionized water was passed at the same flow rate to rinse off HCl.

Adsorption equilibrium experiments were carried out by contacting a given amount of adsorbent with amino acid solution of 1-25 mol/m^3 and organic solvents solution of 200-1,600 mol/m^3 in a constant temperature shaking incubator (298.15 K). The dry base weight of adsorbent was measured after drying for 48 hours in a vacuum oven at 383.15 K. Three days are enough for the system to reach equilibrium. After equilibrium was reached, the excess amino acid left in the solution was analyzed by using UV spectrometry (Varian, model DMS 100s). IPA and methanol concentrations were measured by a GC (Shimadzu, model GC14B), equipped with a hydrogen flame ionization detector. Helium was used as a carrier gas. The adsorption capacity of the polymeric adsorbent was determined from its material balance.

The adsorption column was made of glass with an inside diameter 0.015 m and length 0.3 m. A nonionic polymeric sorbent was packed into the column and sustained by glass beads. A precision micropump regulated the flow rate. The solution was introduced upward into the column. To prevent channeling and to enhance distribution of the solution through the column, the two layers of small glass beads were packed in the top and bottom regions of the column. All the packing procedures were conducted under water to avoid the generation of bubble in the column. After the start of experiments, samples were periodically taken at the determined time intervals by using a fractional collector. The operating conditions of the column are listed in Table 3.

Stock solutions were prepared in a glass tank of 5 L volume, and it was placed in a constant-temperature water bath. The flow was controlled at constant rate with a micrometering pump and the rate was determined with a rotameter during a run. Distilled water was supplied into the column at the same flow rate as the aqueous solution for about 2 hr prior to the start of experiments in order to fill the bed with water and to prevent sudden disturbance of the experimental system at the beginning of the experiments. To maintain the column at constant temperature, 25 °C, a water bath with a temperature controller was used.

Table 3. Experimental conditions for fixed-bed adsorption

Variables	Units	Experimental conditions
Bed length (L)	m	0.05-0.15
Bed diameter (D)	m	0.015
Diameter	mm	0.664
Flow rate (v)	ml/min	2.2, 3, 4
Temperature	°C	25

RESULTS AND DISCUSSION

1. Adsorption Isotherm

Adsorption isotherms are the most fundamental and informative data on an adsorption system. It is also very important for analysis and design of adsorption-based processes. Adsorption onto synthetic adsorbents mainly occurs by the dispersed force between the adsorbate and the resin. Therefore, the adsorption capacity depends on the property of adsorbate, temperature, solution pH, and the amount of impurities contained in the solution.

Table 4. Various isotherms for single components

Name	Model equations	Parameters
Langmuir	$q=\frac{q_m bC}{1+bC}$	q_m, b
Freundlich	$q=k_F C^{1/n}$	k_F, n
Sips	$q=\frac{q_m bC^{1/n}}{1+bC^{1/n}}$	q_m, b, n

Adsorption equilibrium isotherms of two amino acids and two organic solvents on the nonionic polymeric resin, XAD-16, were determined. These experimental isotherms data were correlated by using three well-known isotherm equations such as Langmuir, Freundlich, and Sips. The former two isotherms have two parameters, whereas the latter has three isotherm parameters as listed in Table 4. The parameters were obtained by fitting the data using a modified Levenberg-Marquardt method (IMSL routine DUNSLF). The object function, E (%), represents the average percent deviation between experimental and predicted results as follows:

$$E(\%)=\frac{100}{N}\sum_{k=1}^{N}\left[\frac{q_{exp,k}-q_{cal,k}}{q_{exp,k}}\right] \quad (11)$$

Fig. 1 shows the adsorption equilibrium isotherms of two amino acids on XAD-16. The adsorption capacity for Trp is larger than that for Phe. Adsorption amounts increased with increasing the hydrophobicity. This result suggests that the adsorption amount highly depends on the hydrophobicity of the adsorbates [Ruthven, 1984]. In general, from the economic point of view, the success of an ad-

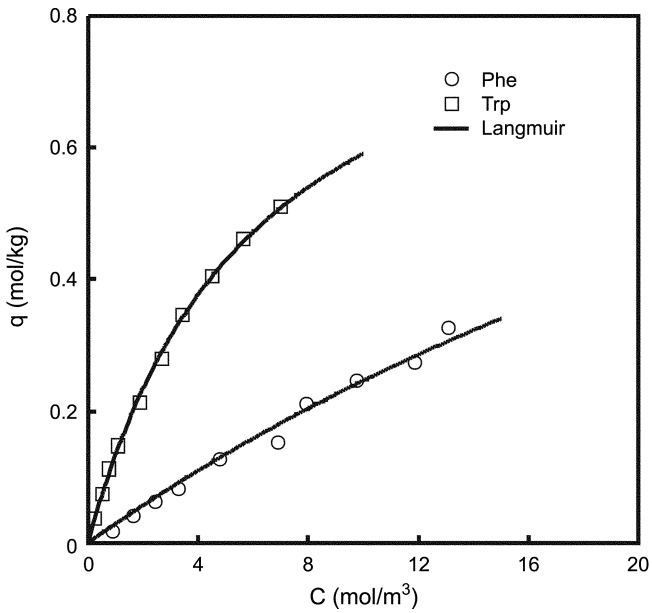

Fig. 1. Adsorption isotherms of Phe and Trp on XAD-16 at 298.15 K.

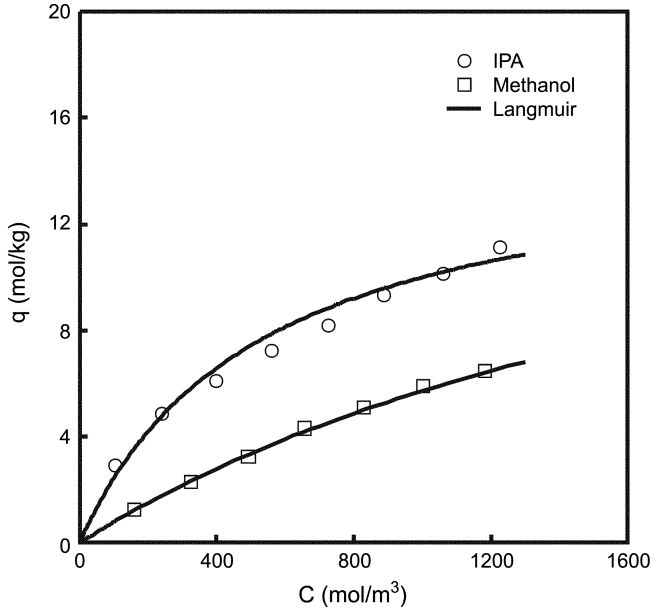

Fig. 2. Adsorption isotherms of IPA and methanol on XAD-16 at 298.15 K.

sorption system usually depends on the regeneration of the sorbent. The choice of desorption method will depend on the physical and chemical characteristics of both the adsorbate and the sorbent. For nonionic polymeric sorbents, the solvent regeneration technique has been considered to be superior to other methods since the attractive forces binding the solute to the resin surface are physical in nature. Fig. 2 shows the adsorption isotherms of IPA and methanol. The affinity of IPA on XAD-16 was greater than that of methanol. Here, the solid lines are the correlated results with the Langmuir isotherm. The isotherm parameters as well as the mean percent deviation error obtained are listed in Table 5.

2. Determination of Model Parameters

In columns packed with porous adsorbents, the major transport parameters are the axial dispersion coefficient, the external film mass transfer coefficient, and the intraparticle diffusion coefficient. When a fluid flows through the packed bed, there is a tendency for axial mixing to occur. Any such mixing is undesirable since it reduces the efficiency of separation. The axial dispersion coefficient depends on the effective intraparticle diffusivity and the magnitude of the concentration gradient through the particle. The effect becomes most significant when all adsorption occurs at the outside of the particle in the initial uptake. Wakao and Funazkri [1976] suggest the following equation as a limiting expression for the system with a rectangular isotherm.

$$\frac{D_L}{2\nu R}=\frac{20}{\xi}\left(\frac{D_m}{2\nu R}\right)+\frac{1}{2}=\frac{20}{ReSc}+\frac{1}{2} \tag{12}$$

External diffusion or film transport controls the transfer of adsorbate from bulk solution through the boundary layer of fluid adjacent to the external surface of the adsorbent. Film transport is governed by molecular diffusion and, in the case of turbulent flow, by eddy, mass, diffusion, which controls the effective thickness of the boundary layer. For spherical particles, the external mass transfer coefficient, k_f, in the column, have been estimated by using the Ranz and Marshall equation [Ruthven, 1984].

$$Sh=\frac{2k_fR}{D_m}=2.0+0.6Re^{0.5}Sc^{0.33} \tag{13}$$

where, Re is the Reynolds number defined as $Re=2R\nu\rho_f/\mu$, Sc is the Schmidt number, $Sc=\mu/D_m\rho_f$, and Sh is the Sherwood number, $Sh=2k_fR/D_m$.

The rate of adsorption by porous adsorbents is generally controlled by the transport within the particle, rather than by the intrinsic kinetics of sorption at the surface. There are various methods for determining the diffusion coefficient in the literature, Here, we determined it by comparing the experimental concentration history in a batch adsorber and the predicted one based on the surface diffusion model by minimizing the object function defined in Eq. (11). The determined values for Phe and Trp are listed in Table 6.

3. Breakthrough Curves under Various Operating Conditions

The performance and operating cost of an adsorption-based separation process greatly depend upon the effectiveness of design and operating conditions. Therefore, rigorous approaches to the design and operation of the adsorption system must be used to ensure efficient and cost effective applications. To do this, one has to understand the mechanism and dynamics of adsorption and desorption as well as major variables, which affect the process performance. Generally, adsorption equilibrium, external and internal mass transfers, and hydrodynamics are needed to simulate the adsorption and desorption behavior in a fixed-bed column.

Figs. 3 and 4 show the single-species breakthrough curves of organic solvents (IPA and methanol) and two amino acids (Phe and Trp) on XAD-16, respectively. The breakthrough time of Phe is earlier than that of Trp, because the affinity of Phe is less than that of Trp. Fig. 5 shows the effect of the bed length on the adsorption of Phe on XAD-16. The experimental results show that the breakthrough curve has a sharper shape when a shorter column is used. Gener-

Table 5. Adsorption isotherm parameters of amino acids and organic solvents on XAD-16 at 298.15 K

Isotherm		XAD-16			
		Phe	Trp	IPA	Methanol
Langmuir	q_m	1.439	0.951	15.169	19.041
	b	0.021	0.164	0.0019	4.3E-4
	E (%)	7.600	3.710	5.796	1.840
Freundlich	k_F	0.0261	0.129	0.243	0.0206
	n	1.0237	1.311	1.875	1.2213
	E (%)	4.4332	6.095	1.561	1.6857
Sips	q_m	2.644	1.229	252.203	52.21
	b	0.009	0.123	0.001	0.0003
	n	0.947	1.110	1.8489	1.1453
	E (%)	6.587	3.328	1.533	1.461

Table 6. Mass transfer coefficient for Phe and Trp within XAD-16 at 298.15 K

	$D_L\times10^6$ [m^2/s]	$k_f\times10^5$ [m/s]	$D_s\times10^{11}$ [m^2/s]
Phe	2.08	7.50	5.82
Trp	1.52	2.50	5.16

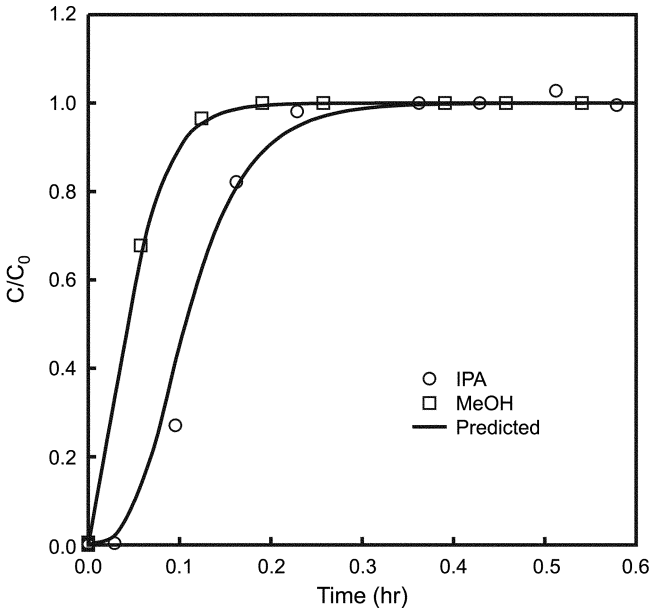

Fig. 3. Breakthrough curves of IPA and methanol on XAD-16 (T= 298.15 K, C_0=10 volume%, v=5.44×10^{-4} m/sec and L=0.10 m).

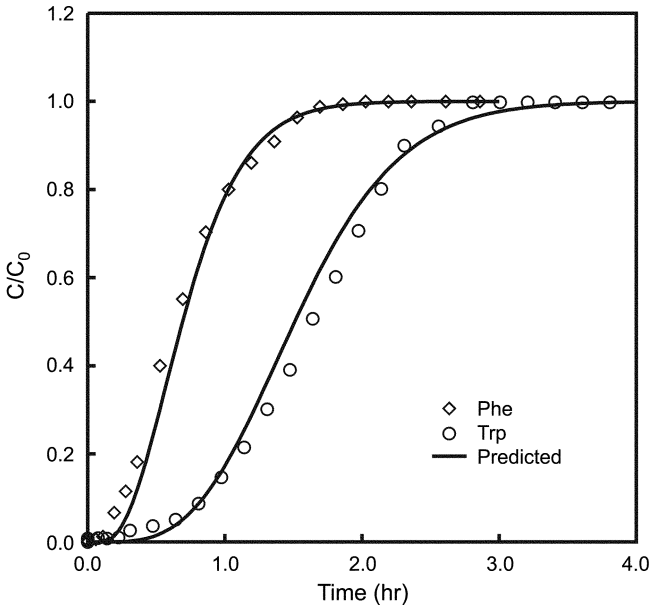

Fig. 4. Breakthrough curves of Phe and Trp on XAD-16 (T=298.15 K, C_0=1 mol/m^3, v=3.99×10^{-4} m/sec, and L=0.10 m).

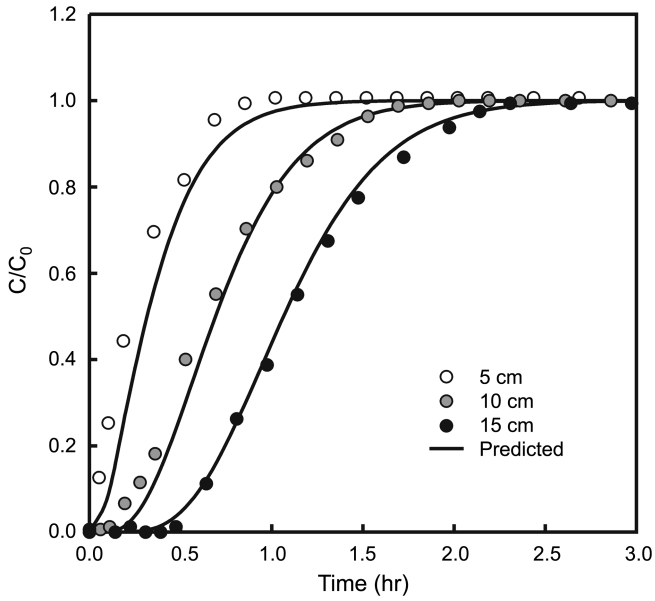

Fig. 5. Effect of bed length on experimental results and model predictions of breakthrough curves on XAD-16 (T=298.15 K, C_0=1 mol/m^3 and v=5.44×10^{-4} m/sec).

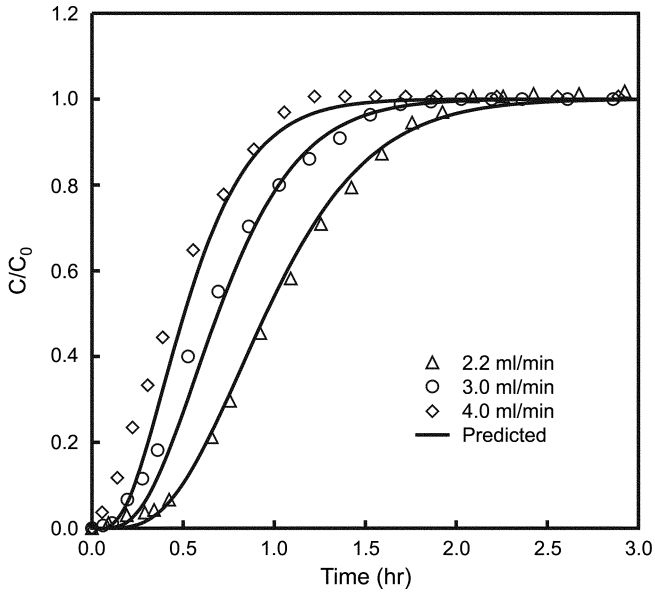

Fig. 6. Effect of flow rate on experimental results and model predictions of breakthrough curves for Phe on XAD-16 (T= 298.15 K, C_0=1 mol/m^3 and L=0.10 m).

ally, this result can be observed when the column length is shorter than the zone length. Since the flow rate is also a very important factor in the column design, its effect should be checked. Fig. 6 shows that the breakthrough appears earlier at higher flow rates. On the other hand, the breakthrough curves are steeper at higher flow rates. In general, if the flow rate is decreased or the bed length increased, the breakthrough curve becomes steeper. However, the results obtained here show contrary tendencies, which can be explained by two reasons: the almost linear single component adsorption isotherm and the film mass transfer controlling. Fig. 7 also shows that breakthrough curves are marginally influenced by initial concentrations since the isotherm is almost linear as shown in Fig. 1.

The success of an adsorption process usually depends on the regeneration step of the adsorbent from the economic point of view. Regeneration of the adsorbed solute from the adsorbent has been accomplished by one of two general methods. One is to change a physical operating condition, namely temperature, of the adsorber, which affects the equilibrium interaction between the adsorbent and the solute. The other is to perform a chemical reaction in the adsorber to change the nature of the adsorbed component so it can be

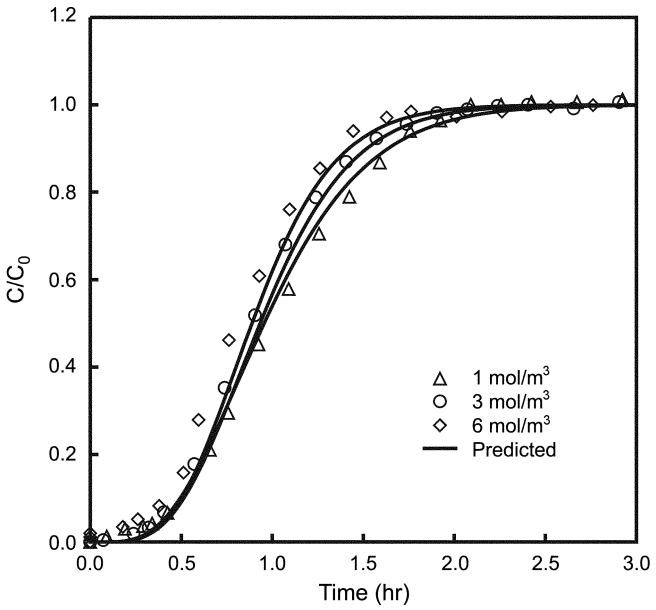

Fig. 7. Effect of initial concentration on experimental results and model predictions of breakthrough curves for Phe on XAD-16 (T=298.15 K, v=5.44×10^{-4} m/sec and L=0.10 m).

desorbed and removed from the system readily. In general, there are many regeneration techniques such as thermal, steam, acid, base, and solvent regenerations. The choice of a certain regeneration method will depend upon the physical and chemical characteristics of both the adsorbate and the adsorbent. For nonionic polymeric adsorbents, the solvent regeneration technique has been known to be superior to other methods since the attractive forces binding the solute to the resin surface are physical in nature. The solvent regeneration of polymeric adsorbents is particularly effective when the components adsorbed are very soluble in the solvent and the solvating force is much greater than the physical adsorptive force holding the adsorbate onto the resin. Most solvents are adsorbed by polymeric adsorbents and in many cases they penetrate the gel phase of the polymeric matrix. This results in the solvent displacement of the component adsorbed in the resin. In this study, IPA and methanol were used as a desorbate for amino acids.

Figs. 8 and 9 show the adsorption and desorption breakthrough curves to check the effect of IPA and methanol on them. As the con-

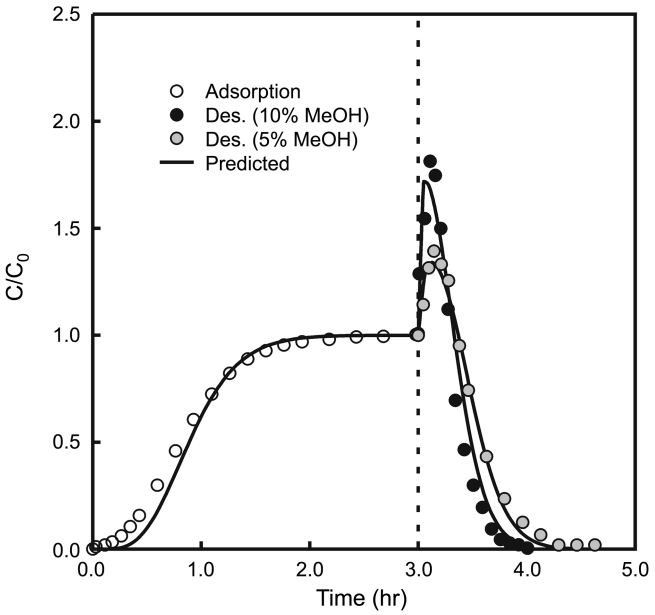

Fig. 9. Effect of methanol concentration on adsorption and desorption breakthrough curves for Phe on XAD-16 (C_0=6 mol/m^3, v=3.99×10^{-4} m/sec and L=0.10 m).

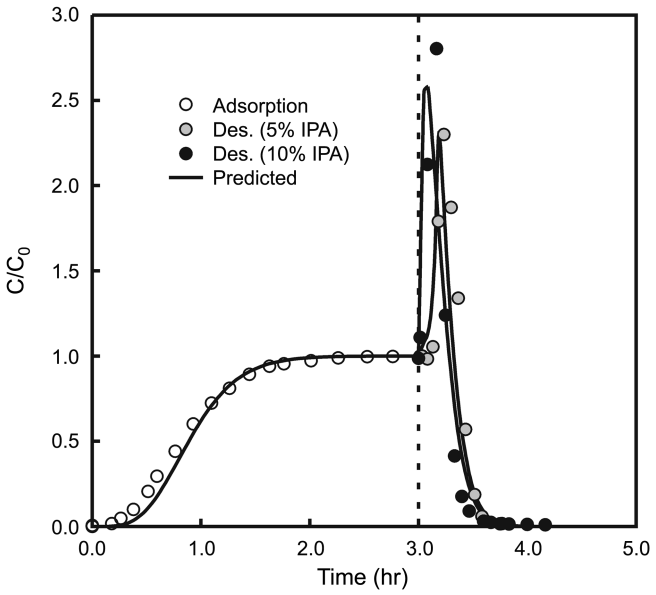

Fig. 8. Effect of IPA concentration on desorption breakthrough curves for Phe on XAD-16 (C_0=6 mol/m^3, v=3.99×10^{-4} m/sec and L=0.10 m).

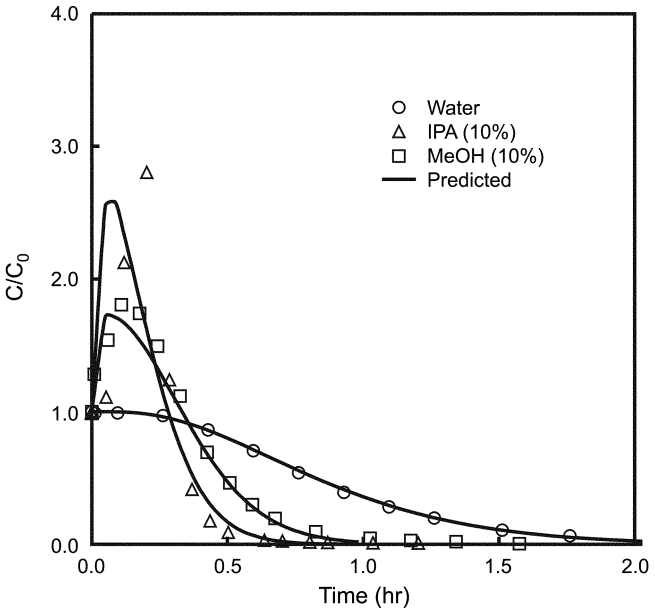

Fig. 10. Effect of organic solvents on desorption breakthrough curves for Phe on XAD-16 (C_0=6 mol/m^3, pH=5.30, v=3.99×10^{-4} m/sec and L=0.10 m).

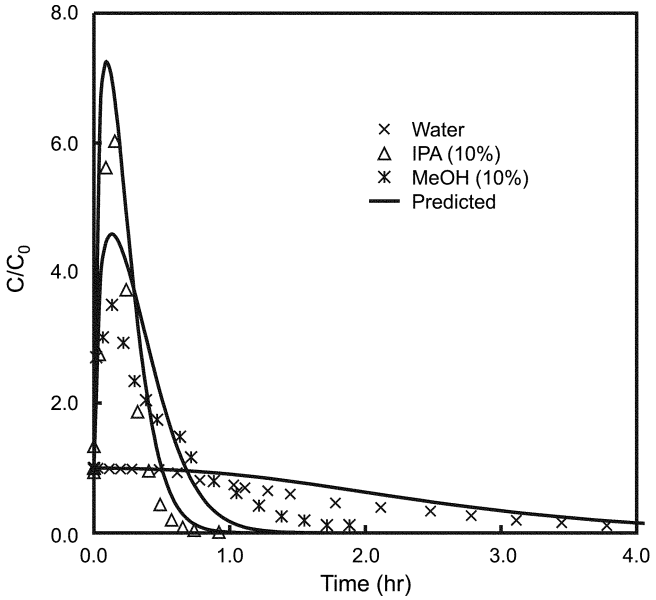

Fig. 11. Effect of organic solvents on desorption breakthrough curves for Trp on XAD-16 (C_0=1 mol/m^3, pH=5.30, v=4.54 ×10^{-4} m/sec and L=0.10 m).

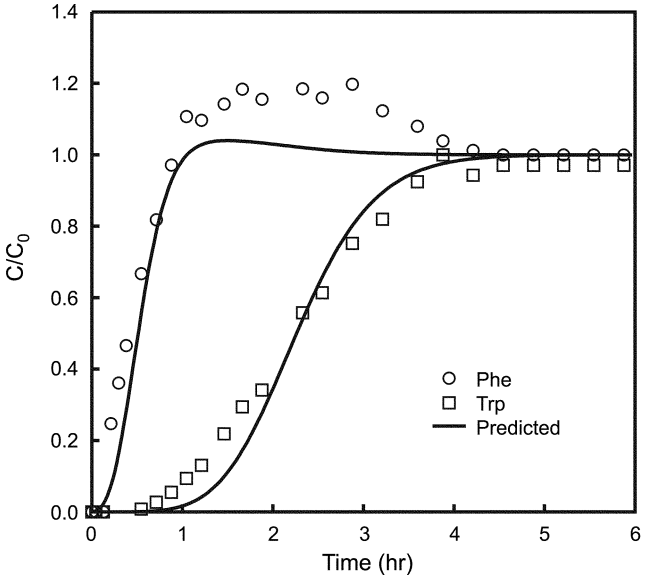

Fig. 12. Prediction and experimental results of binary breakthrough curves of Phe/Trp on XAD-16 (C_{Phe}=3 mol/m^3, C_{Trp} =1.5 mol/m^3 v=4.54×10^{-4} m/sec and L=0.10 m).

centrations of IPA and methanol in the regeneration solution increase, the overshoot in the desorption curve becomes higher and desorption occurs quickly. Also, removal efficiency of Trp is greater than that of Phe under the same experimental conditions. If the excess amount of IPA does not cause trouble in the further process to separate amino acids from the mixture with IPA, a higher concentration of IPA may be used to perform the regeneration step more effectively. The high regeneration efficiency of IPA results from the contribution of solubility and affinity differences.

Figs. 10 and 11 show the comparison of the same concentration of organic solvents in desorption. The predicted breakthrough curves were obtained by using the proposed model, without any adjustment of model parameters. Each figure shows an adsorption breakthrough curve and three desorption curves obtained with 10% aqueous solutions of IPA and methanol and with only deionized water, respectively. The effect of IPA on desorption is better than that of other desorbates because the adsorption affinity is very high. Even when pure water without IPA was introduced into the column, amino acids were desorbed quite well but it took longer. It should be noted that when one uses an organic solvent to regenerate the adsorbent, additional cost will be required to separate the mixture of amino acids and IPA in the next step. Finally, we measured binary breakthrough curves of Phe and Trp in the XAD-16 column as shown in Fig. 12 and predicted the corresponding theoretical breakthrough curves for comparison. According to the result, it seems that the simple dynamic model suggested here works reasonably well for binary systems.

CONCLUDING REMARKS

As a separation and purification method for amino acids dissolved in aqueous solutions, the adsorption and desorption behaviors of amino acids on a nonionic polymeric adsorbent, XAD-16, were investigated in a fixed bed column under various operating conditions such as concentration, flow rate, and column length. Pure component adsorption equilibrium data of amino acids and organic solvents were fitted with three well-known isotherms. In particular, it is known that the Langmuir equation fits all single component data reasonably well. The desorption of amino acids from the resin by using IPA and methanol was described reasonably by a competitive adsorption model, the ideal adsorbed solution theory based on the Langmuir equation as single component isotherms.

According to the column experiments, the breakthrough of amino acids appeared earlier but became steeper at high flow rates. On the other hand, the breakthrough curves were not so influenced by initial concentrations. These imply that the results obtained here show contrary tendencies, compared to general cases. The reasons for this result seem to be that adsorption isotherms are almost linear and the film mass transfer controls the mass transport. Furthermore, the proposed simple dynamic model successfully simulated experimental adsorption and desorption breakthrough behavior of Phe and Trp under various operating conditions. Therefore, it could be concluded that the proposed model can be used for the design of a cyclic operation that employs a column charged with polymeric adsorbents. In addition, it was found that the cyclic separation method using the polymeric resin could be a promising technique for this purpose.

ACKNOWLEDGMENT

This work was supported by Chonnam National University under the program of 2000-sabbatical-year for H. Moon.

NOMENCLATURE

AS : collocation coefficient of the first derivative for particles [-]

AF : collocation coefficient of the first derivative for the column [-]
BS : collocation coefficient of the second derivative for particles [-]
BF : collocation coefficient of the second derivative for the column [-]
b : Langmuir or Sips constant [mol/m^3]
C : concentration in the fluid phase [mol/m^3]
C_s : concentration in equilibrium with the adsorbed phase [mol/m^3]
D : column diameter [m]
D_L : axial dispersion coefficient [m^2/s]
D_m : molecular diffusion coefficient [m^2/s]
D_s : surface diffusion coefficient [m^2/s]
E : percent error [%]
k_f : film mass transfer coefficient [m/s]
k_F : Freundlich constant [mol/kg]
L : column length [m]
n : Sips constant [-]
N : number of data point [-]
NTE : number of total finite elements [-]
NTF : number of total interior collocation points in the column [-]
NTS : number of total interior collocation points in the particles [-]
q : concentration in particle phase [mol/kg]
q_m : Langmuir or Sips constant [mol/kg]
r : radial distance [m]
R : particle radius [m]
t : time [s]
X : dimensionless radial distance [-]
z : dimensionless bed height [-]
Δz : grid size

Greek Letters

α : dimensionless group defined by $k_f R/D_s$
ε_b : column porosity
η : dimensionless group defined by $(1-\varepsilon_b)/\varepsilon_b$
θ : dimensionless group defined by $vR^2\varepsilon_b/LD_s(1-\varepsilon_b)$
ρ_p : particle density [kg/m^3]
ρ_f : fluid density [kg/m^3]
τ : dimensionless time defined by $D_s t/R^2$
v : interstitial velocity [m/s]
ξ : void fraction in a fixed bed system

Superscripts and Subscripts

i, j : collocation points
k : section
L : component
exp : experimental
pre : predicted

Abbreviation

b : bed
conc : concentration
p : particle
Pe : Peclet number
Re : Reynolds number
Sc : Schmidt number
Sh : Sherwood number

REFERENCES

Carta, G., Saunders, M. S., DeCarli, J. P. and Vierow, J. B., "Dynamics of Fixed-bed Separations of Amino Acids by Ion Exchang," *AIChE Symp. Ser.*, **84**, 54 (1998).

Costa, C. and Rodrigues, A. E., "Design of Cyclic Fixed Bed Adsorption Process. Part I. Phenol Adsorption on Polymeric Adsorbents," *AIChE J.*, **31**, 1645 (1985).

Diez, S., Leitao, A., Ferreira, L. and Rodrigues, A., "Adsorption of Phenylalanine onto Polymeric Resins: Equilibrium, Kinetics and Operation of a Parametric Pumping Unit," *Sep. Purif. Technol.*, **13**, 25 (1998).

Doulia, D., Rigas, F. and Gimouhopoulos, C., "Removal of Amino Acids from Water by Adsorption on Polystyrene Resins," *J. Chem. Technol. Biotechnol.*, **76**, 83 (2001).

Dutta, M., Baruah, R. and Dutta, N. N., "Adsorption of 6-aminopenicillanic Acid on Activated Carbon," *Sep. Purif. Technol.*, **12**, 99 (1997).

Grzegorczyk, D. J. and Carta, G., "Adsorption of Amino Acids on Porous Polymeric Adsorbents-I. Equilibrium," *Chem. Eng. Sci.*, **51**, 807 (1996).

Kubota, L. T., Gambero, A., Santos, A. S. and Granjeiro, J. M., "Study of the Adsorption of Some Amino Acids by Silica Chemically Modified with Aminobenzenesulfonic and Phosphate Groups," *J. Col. Inter.*, **183**, 453 (1996).

Lee, J. W., Park, H. C. and Moon, H., "Adsorption and Desorption of Cephalosporin C on Nonionic Polymeric Sorbents," *Sep. Purif. Technol.*, **12**, 1 (1997a).

Lee, J. W., Jung, H. J. and Moon, H., "Effect of Operating Conditions on Adsorption of Cephalosporin C in a Column Adsorber," *Korean J. Chem. Eng.*, **14**, 277 (1997b).

Lee, J. W. and Moon, H., "Effect of pH on Adsorption of Cephalosporin C by a Nonionic Polymeric Sorbent," *Adsorption*, **5**, 381 (1999).

Melis, S., Markos, J., Cao, G. and Mobidelli, M., "Ion-exchange Equilibria of Amino Acids on a Strong Acid Resin," *Ind. Eng. Chem. Res.*, **35**, 1912 (1996).

Moitra, S., Mundhara, G. L. and Tiwari, J. S., "Studies of the Sorption Behaviour of Some Amino Acids on Chemically Pretreated Alumina in Relation to Chromatography," *Colloids and Surfaces*, **41**, 311 (1998).

Myers, A. L. and Prausnitz, J. M., "Thermodynamics of Mixed Gas Adsorption," *AIChE J.*, **11**, 121 (1965).

Park, I. S., "Numerical Analysis of Fixed Bed Adsorption Kinetics Using Orthogonal Collocation," *Korean J. Chem. Eng.*, **19**, 1001 (2002).

Podlesnyuk, V. V., Hradil, J. and Králová, E., "Sorption of Organic Vapors by Macroporous and Hypercrosslinked Polymeric Adsorbents," *Reac. Func. Poly.*, **42**, 181 (1999).

Ruthven, D. M., "Principles of Adsorption and Adsorption Processes," John Wiley and Sons, New York (1984).

Villadsen, J. and Michelsen, M. L., "Solution of Differential Equation Models by Polynomial Approximation," Prentice-Hall, Englewood Cliffs, NJ (1978).

Wakao, N. and Funazkri, "Effect of Fluid Dispersion Coefficient on Particle to Fluid Mass Transfer Coefficients in Packed Beds Correlation of Sherwood Numbers," *Chem. Eng. Sci.*, **33**, 1375 (1978).